Araştırma Makalesi / Research Article

Molten Salt Approach for Co₃O₄ Synthesis as a Charge Storage Electrode

Ümran KURTAN[1*]

[1] *Department of Materials and Materials Processing Technologies, Vocational School of Technical Sciences, İstanbul University-Cerrahpaşa, 34500, İstanbul/Turkey*

Corresponding author e-mail: umran.kurtan@iuc.edu.tr   ORCID ID: http://orcid.org/0000-0002-1279-7729

Keywords
Molten Salt Method;
Cobalt Oxide;
Electrode;
Energy Storage

Abstract

A versatile molten salt method was targeted to fabricate the cobalt oxide (Co₃O₄) nanospheres as charge storage electrodes. The Co₃O₄ nanospheres were prepared in KNO₃ molten salt in only one step within 5 minutes. The nanospheres were with an average size distribution of almost 80-130 nm. The specific capacitance of cobalt oxide was found to be 285 F/g at 10 mV/s and 171 F/g at 0.5 A /g in 6 M KOH and the Trasatti method was used to understand the outer and inner surface capacitive contributions. The material possessed a moderate rate capability (63.1% at 5 A/g) and had good cyclic stability (90.5% after 1200 cycles). This experimental study does not require any solvent usage and thus can provide a green and continuous approach for the preparation of various transition metal oxides with good electrochemical properties in the energy storage field.

Bir Yük Depolama Elektrodu Olarak Co₃O₄ Sentezi İçin Eriyik Tuz Yaklaşımı

Anahtar Kelimeler
Eriyik Tuz Yöntemi;
Kobalt Oksit;
Elektrot;
Enerji Depolama

Öz

Yük depolama elektrotları olarak kobalt oksit (Co₃O₄) nanokürelerini sentezlemek için çok yönlü bir eriyik tuz yöntemi hedeflenmiştir. Co₃O₄ nanoküreleri KNO₃ erimiş tuzunda sadece tek adımda 5 dakika içerisinde hazırlanmıştır. Nanokürelerin ortalama boyut dağılımı yaklaşık 80-130 nm'dir. Kobalt oksidin spesifik kapasitansı 6 M KOH elektrolitinde 10 mV/s'de 285 F/g ve 0.5 A/g'da 171 F/g olarak bulunmuş ve dış ve iç yüzey kapasitif katkılarını anlamak için Trasatti yöntemi kullanılmıştır. Malzeme orta seviyede bir kapasite koruması (5 A/g'da %63.1) ve iyi bir döngüsel kararlılık (1200 çevrim sonrası %90.5) göstermiştir. Bu deneysel çalışma herhangi bir çözücü kullanımını gerektirmemektedir ve bu nedenle enerji depolama alanında iyi elektrokimyasal özelliklere sahip çeşitli geçiş metal oksitlerinin hazırlanması için yeşil ve sürekli bir yaklaşım sağlayabilir.

© Afyon Kocatepe Üniversitesi

1.   Introduction

As promising energy storage devices, supercapacitors are of special significance because of their good specific power, long cycle life, and rapid charge/discharge process. Supercapacitors also called ultracapacitors or electrochemical capacitors are used in many fields including electric vehicles, portable electronic power systems, and military service (Kurtan 2022, Kurtan and Aydın 2021, Lee *et al*. 2011, Wang *et al*. 2010). An electrode is a critical component of supercapacitors and transition metal oxides such as Co₃O₄ (Kebabsa *et al*. 2020, Tan *et al*. 2015), MnO₂ (Du *et al*. 2022),

NiO (Liang *et al*. 2012), V₂O₅ (Kim *et al*. 2013) and ZnO (Ma *et al.* 2020) have been considered as potential high capacitance electrodes due to their facile availabilities. Among these, Co₃O₄ is attractive, and sensors, catalysts, magnetic resonance imaging, lithium-ion batteries, and supercapacitors are the possible application areas of cobalt oxide. Owing to its many advantages such as earth-abundance, being environmentally friendly, low cost, and multiple valence states, it gained significant attention in the energy storage field, specifically supercapacitors. Up to now, traditional methods including solution combustion (Afrooze and Shaik

2023), sol-gel (Priyadharsini *et al.* 2020), hydrothermal (Anuradha and Raji 2022, Arjunan *et al.* 2023), solvothermal (UmaSudharshini *et al.* 2021, Gao *et al.* 2023), electrodeposition (Jadhav *et al.* 2023) and reflux (Packiaraj *et al.* 2019) have been utilized to prepare a variety of cobalt oxide nanostructures. However, these reported preparation methods not only require multi-steps but also are complicated and time-consuming. In addition to these methods, molten-salt synthesis is one of the simple, cheap, and non-toxic method to obtain high-quality nanomaterials in a relative temperature and time. It can overcome all these drawbacks since it is facile (one-step), ultrafast, and does not require any solvent usage. Moreover, the sealing is not necessary for the experiment resulting in large amounts of electrodes that can be easily fabricated.

In this study, the main goal is to synthesize porous Co_3O_4 nanomaterial as a potential supercapacitor electrode by a versatile molten-salt method. It is well-known that there is a close relationship between the starting material and the as-synthesized Co_3O_4 nanostructures. Cobalt (II) sulfate heptahydrate ($CoSO_4.7H_2O$) was used as a precursor with a low melting temperature (96.8 °C). The reaction occurred at a relative temperature of 380 °C which is necessary for the melting of KNO_3 salt in the air atmosphere. The inorganic salt served as both a template and an activating agent. Any further calcination or physical and chemical treatments have been used. This facile approach can save cost and gain insight into the large-scale production of electrode materials for supercapacitors and other energy storage devices compared with traditional techniques.

2. Experimental

2.1. Material Synthesis

The 5 g of KNO_3 salt in a crucible was heated to 380 °C in a furnace until a molten state was reached. Then, the crucible was taken and 3.6 mmol cobalt (II) sulfate heptahydrate ($CoSO_4.7H_2O$) was added into the molten salt, which was maintained for 5 min in the furnace. The black product was taken and cooled down naturally. Finally, washing was done with hot distilled water to remove recrystallized KNO_3 salt. The preparation step of the Co_3O_4 nanospheres is illustrated in Fig. 1.
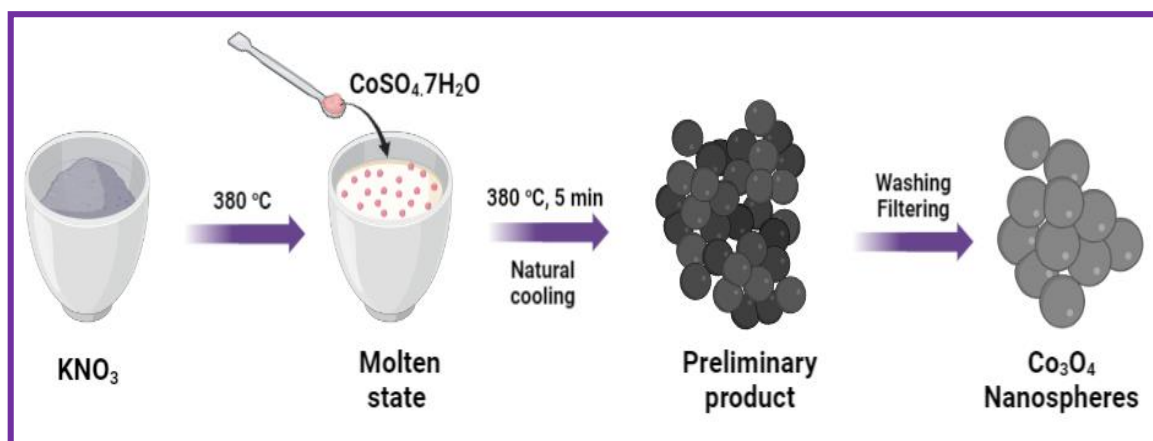
Fig. 1. Representation of the synthesis of Co₃O₄.

2.2. Material Characterizations

The morphological properties were investigated by scanning electron microscopy (SEM) with an FEI Quanta 250 FEG instrument and transmission electron microscopy (TEM, Hitachi HT-7700, 40-120 kV). X-ray diffraction (XRD) pattern was recorded on a Thermo Scientific ARL X'TRA, and FTIR was measured with a Bruker Alpha instrument.

2.3. Electrode Preparation and Electrochemical Measurements

The as-synthesized Co_3O_4 nanosphere (80 wt%), carbon black (10 wt%), and polyvinylidene difluoride

(PVDF) (10 wt%) were mixed in a few drops of N-methyl-2-pyrrolidone (NMP). Then, it was coated onto a Ni foam followed by drying at 100 °C for 12 h. Approximately 3.7 mg of electroactive material with an area of 1 cm^2 was coated. The electrochemical behaviours were investigated using a three-electrode system. Co₃O₄ nanospheres, Ag/AgCl, and Pt were used as the working, reference, and counter electrode, respectively. 6 M KOH was the electrolyte, and the electrochemical tests of the electrode were analyzed by cyclic voltammetry (CV), galvanostatic charge-discharge (GCD), and the electrochemical impedance spectroscopy (EIS) techniques using the GAMRY Reference 3000. EIS was measured in a frequency scale of 100 kHz-0.1 Hz at open circuit potential. The specific capacitances from CV and GCD analysis can be calculated by using the following equations, respectively (Liu *et al.* 2012, Üstün *et al.* 2023, Zhang *et al.* 2014).

$$C = \frac{\int_{V_1}^{V_2} I dV}{mv\Delta V} \qquad (1)$$

$$C = I\Delta t / m\Delta V \qquad (2)$$

where C is the gravimetric specific capacitance (F/g), I is the current (A), m is the mass of the electrode, *v* is the scan rate, and ΔV is the potential interval.

3.   Results and Discussion

The morphological character of Co₃O₄ was depicted and shown in Fig. 2a-c. The obtained Co₃O₄ possessed spherical shape morphology with an average particle size distribution of almost 80-130 nm. The energy dispersive X-ray (EDX) was shown in Fig. 2d and the atomic percentages of cobalt and oxygen elements were 90.61% and 9.39%, respectively. The SEM image (Fig. 3a) with the corresponding elemental mapping images in Fig. 3b demonstrated that cobalt and oxygen elements existed and were homogeneously distributed throughout the Co₃O₄ nanospheres. The morphology of the Co₃O₄ was further investigated using TEM analysis (Fig. 3c and 3d) and it can be seen

that the particles were relatively agglomerated. The spherical structure was clearly observed which provides a continuous pathway for ion transfer. The crystallinity was investigated by XRD and the spectrum of Co₃O₄ nanospheres was seen in Fig. 4a. The diffraction peaks at 18.8°, 30.8°, 35.8°, 43.8°, 55.6°, 58.2°, 66.3°and 76.4° were attributed to the crystal planes of (111), (202), (311), (400), (422), (333), (404) and (022) which matches the JCPDS data (Card No. 96-900-5892). It is notable that peaks were intense and sharp which reveals the good crystalline structure of Co₃O₄, with no traces of other phases or impurities. The crystallite size of the sample was calculated by Scherer's equation and was found as ~16.8 nm. Low crystallite size can make the ion transfer path easier and decrease the charge transfer. The FTIR spectrum is represented in Fig. 4b. Two characteristic and intense peaks were observed at 550 and 656 cm^{-1}, which are related to the stretching vibrations of the Co–O bonds. The band at 550 cm^{-1} is responsible for the vibration of the Co^{3+}–O while the band at 656 cm^{-1} belongs to the Co^{2+}–O the Co₃O₄ nanospheres (Liu *et al.* 2017, Tharasan *et al.* 2022). The broad band in the range of 3000-3700 cm^{-1} can be attributed to the stretching vibrations of hydroxyl group and the peak at 1200 cm^{-1} can be attributed to carbonates resulting from the reaction of cobalt oxide with carbon dioxide in the air during the synthesis (Guo *et al.* 2018, Tharasan *et al.* 2022). FTIR analysis verified the formation of cobalt oxide.
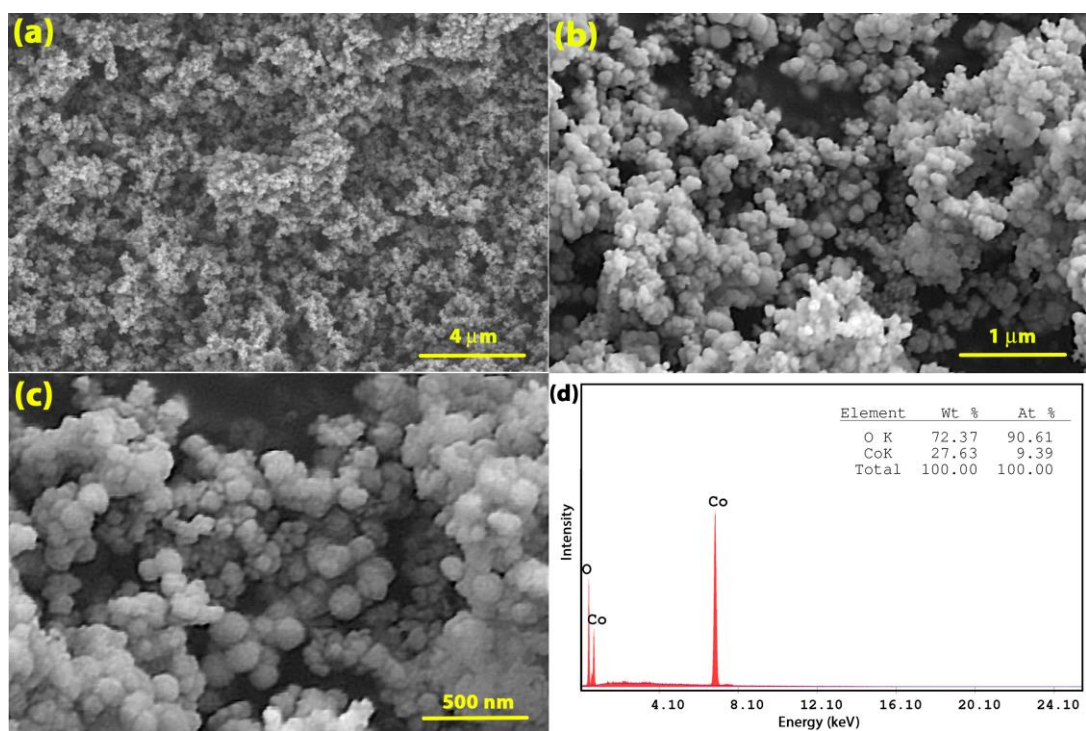
Fig. 2. (a-c) SEM images of Co$_3$O$_4$ (d) EDX spectrum.
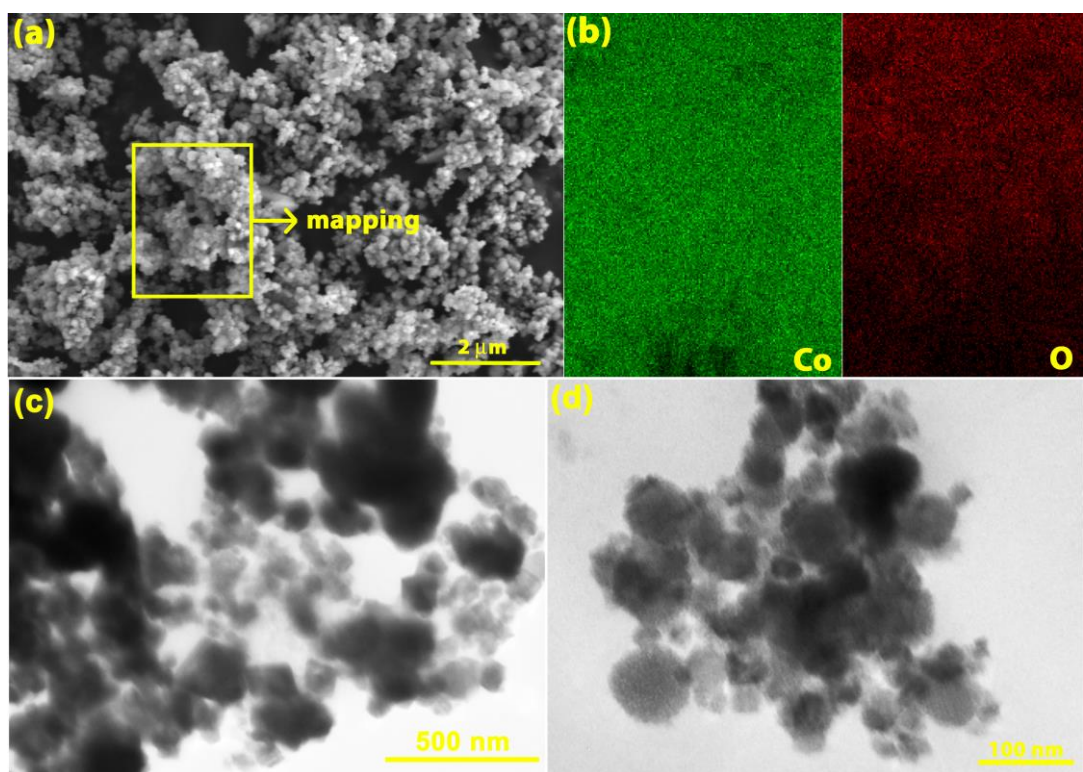
Fig. 3. (a) SEM image, **(b)** the EDX mapping images of Co and O elements, **(c)** low magnification, and **(d)** high magnification of TEM images of Co$_3$O$_4$ nanospheres.

a

b
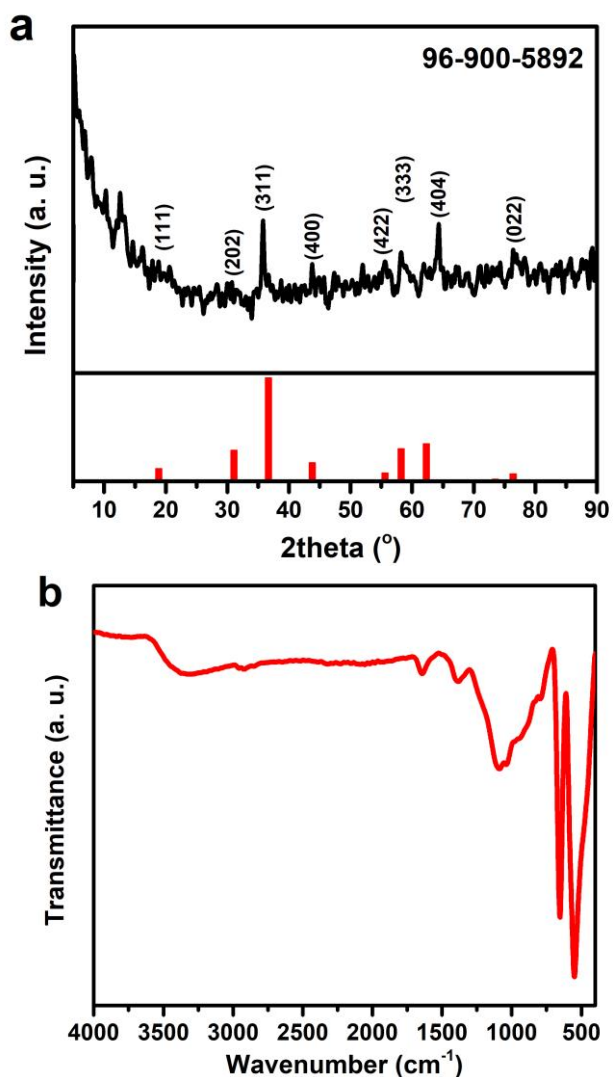
Fig. 4. (a) The XRD pattern and **(b)** FTIR spectra of Co₃O₄.

Fig. 5a displays the CV curves between 0 to 0.4 V (vs. Ag/AgCl) with various scan rates from 10 to 200 mV/s. During scanning, a pair of distinct redox peaks were seen which is ascribed to the reversible redox reaction of Co^{+3}/Co^{+2} and reveals the pseudocapacitance behaviour (Yang *et al.* 2013). The energy storage mechanism requires two essential steps including non-faradic and faradic processes as shown in the following (Chen *et al.* 2019, Liu *et al.* 2017, Wang *et al.* 2016):

Non-faradic:

$$Co_3O_4(surf.) + OH^- \leftrightarrow Co_3O_4(OH^-)surf. \quad (3)$$

Faradic:

$$Co_3O_4 + OH^- + H_2O \leftrightarrow 3CoOOH + e^- \quad (4)$$

$$CoOOH + OH^- \leftrightarrow CoO_2 + H_2O + e^- \quad (5)$$
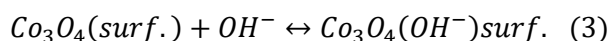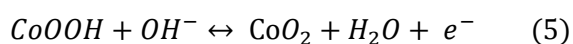
It was also observed that oxidation peaks were not completely symmetric with reduction peaks which is probably due to the polarization of the electrode and the solution resistance during faradic processes (Liu *et al.* 2017, Meher *et al.* 2011, Vidhyadharan *et al.* 2014). Fig. 5b shows the specific capacitance (F/g) versus scan rate (mV/s) and the values reduced with the increase in scan rate. Because at high scan rates, only the outer surface can be used and electrolyte cannot go into the inside of the electrode due to limited time. The specific capacitance for Co₃O₄ was found to be 285 F/g at 10 mV/s and 155 F/g at 200 mV/s, which is a good rate capability of 54.4%.

a

b
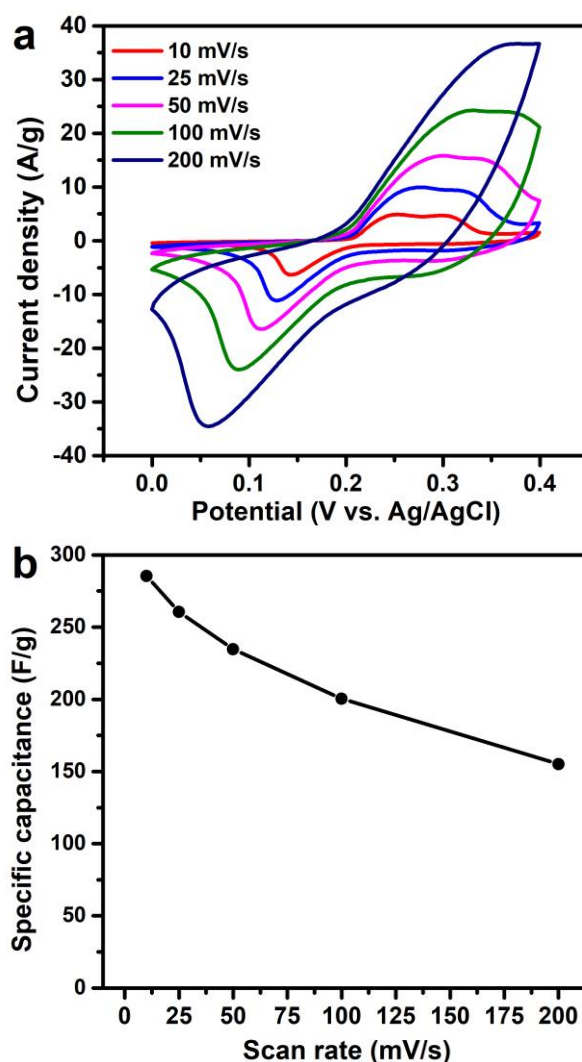
Fig. 5. (a) CV curves and, **(b)** Specific capacitances for different scan rates.

In order to distinguish capacitive contributions of the total capacitance, the Trasatti method has been used (Ardizzone *et al.* 1990). First, CVs of Co₃O₄ were collected for different scan rates. The total

capacitance (C_{total}) is the summation of the outer and inner surface capacitances which depend on the scan rate as in the following:

$$C_{total} = C_{outer} + C_{inner} \ (F/g) \qquad (6)$$

At a high scan rate, the accumulation results from the outside of the electrode while both inside and outside accumulation can be occurred only at low scan rates. The total capacitance can be defined as the following:

$$C^{-1}(v) = constant(v^{0.5}) + C_{total}^{-1} \qquad (7)$$

where v is the scan rate. Plotting $C^{-1}(v)$ versus $v^{0.5}$ gives a linear graph (Fig. 6a). When the linear fit to the y-axis (C vs $v^{-0.5}$) was extrapolated, a new linear graph can be drawn as seen in the following formula (Fig. 6b):

$$C(v) = constant(v^{-0.5}) + C_{outer} \qquad (8)$$

Subtraction of C_{outer} from C_T gives the C_{inner}. As a result, the capacitive contributions of inner and outer surfaces were found as 50.9% and 49.1%, respectively (Fig. 6c).
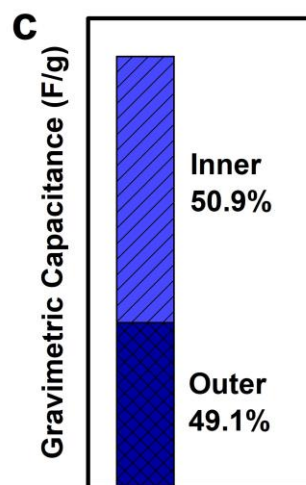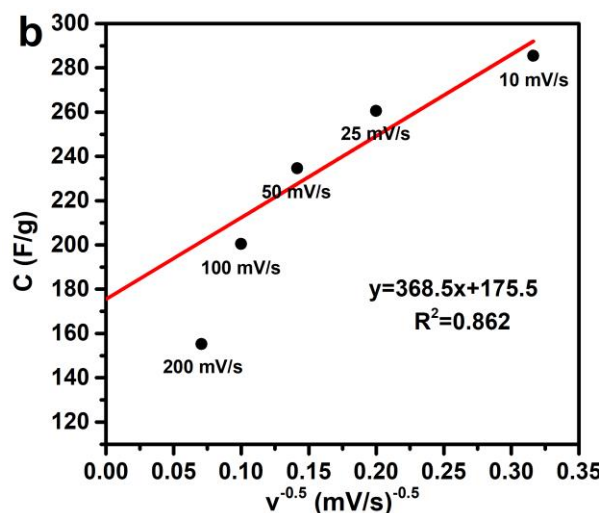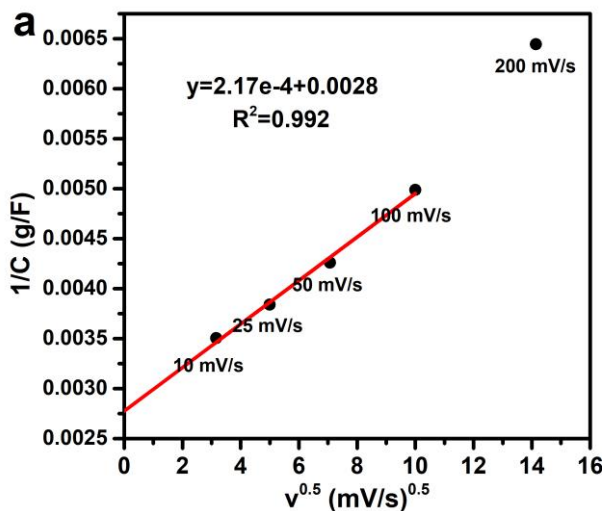
Fig. 6. (a) Plot of 1/C vs $v^{0.5}$, **(b)** C vs $v^{-0.5}$, and **(c)** histogram of capacitance contribution.

Fig. 7a shows the GCD curves in the range of 0 to 0.4 V (Vs Ag/AgCl). The specific capacitance was 171 F/g at 0.5 A/g and sustained its rate performance of 63.1% at 5 A/g, which is much higher than many recent studies in the literature (Table 1) (Afrooze and Shaik 2023, Lima-Tenório *et al.* 2018, Pore *et al.* 202, Priyadharsini *et al.* 2020, Tharasan *et al.* 2022, Tummala *et al.* 2012; Wang *et al.* 2011). The calculated specific capacitances of Co₃O₄ for all current densities and various scan rates are shown in Table 2. Moreover, the cyclic ability of Co₃O₄ at 2 A/g after 1200 cycles was found to be 90.5% which demonstrates its remarkable rate performance (Fig. 7b).

Table 1. Comparison of the Co_3O_4 electrode with some other Co_3O_4 nanostructures in the literature.

Materials	Synthesis Method	Time	Temp.	Electrolyte	Capacitance	Potential (V)	Cycling Stability	Ref.
Co_3O_4 nanosphere	**Molten Salt**	**5 min**	**380°**	**6 M KOH**	**171 F/g (0.5 A/g)**	**0-0.4**	**90.5%-1200**	**This Study**
Co_3O_4 nanosphere	Combustion	1h+8h	150°	1 M KOH	182 F/g (0.5 A/g)	0-0.7	71%-2000	(Afrooze and Shaik 2023)
Co_3O_4 NPs	Precipitation	2h+3h	80-400°	6 M KOH	115.3 F/g (1 A/g)	-0.1-0.45	No change	(Tharasan *et al.* 2022)
Co_3O_4 NPs	Sol-Gel	2h	400°	1 M KOH	120 F/g (1mA/cm^2)	0-0.6	-	(Lima-Tenório *et al.* 2018)
Co_3O_4 microflakes	Hydrothermal	18h+2h	453-673K	1 M KOH	127 F/g (0.1 mA/cm^2)	0-0.45	95.6%-1000	(Pore *et al.* 2021)
Co_3O_4-layered	Precipitation	3h	400°	2 M KOH	202.5 F/g (1 A/g)	0-0.4	82%-2000	(Wang *et al.* 2011)
Co_3O_4	Plasma Spray	-	-	6 M KOH	162 F/g (2.75 A/g)	~0-0.35	72.2%-1000	(Tummala *et al.* 2012)
Co_3O_4 microspheres	Solvothermal	16h+2h	120°+350°	3 M KOH	261.1 F/g (0.5 A/g)	~0-0.37	90.2%-2000	(Guo *et al.* 2018)
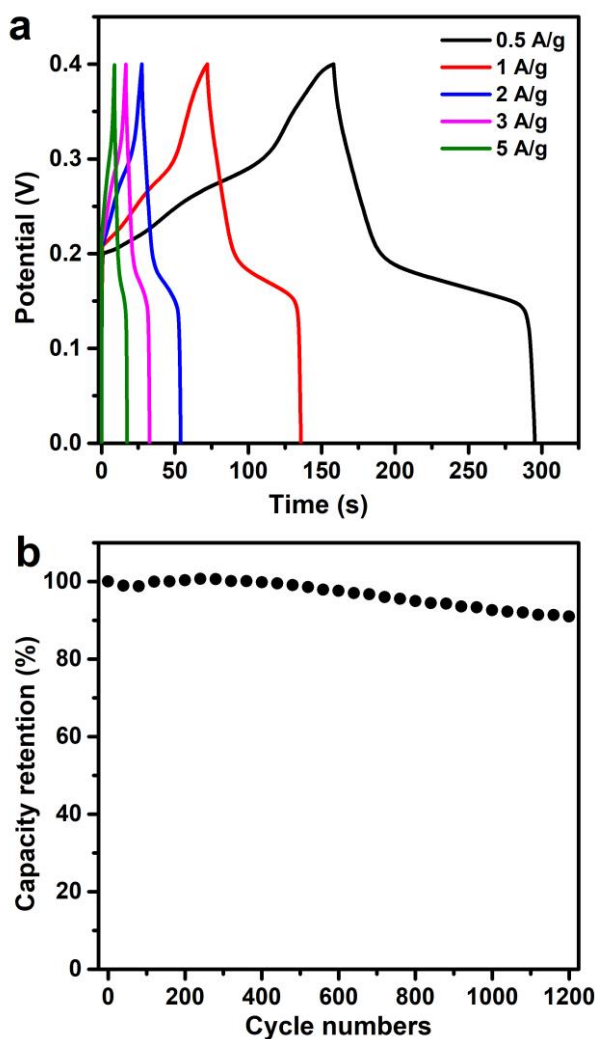
Fig. 7. (a) GCD curves and **(b)** Cyclic performance at 2 A/g of the Co_3O_4.

Fig. 8a shows the EIS spectra and its equivalent circuit inset which includes the series resistance (Rs), and charge transfer resistance (Rct). Low resistance values were seen which indicate good conductivity of the Co_3O_4 nanospheres. Warburg impedance (W) resulting from the frequency dependence of ion diffusion into the electrode, the capacitance (C) of the electrode, and constant phase angle (Q) are the other circuit parameters. Fig. 8b is the Bode diagram which gives information about the relaxation time ('t_0'). It is the inverse of the frequency (f_0) when the phase angle is -45° ($t_0 = 1/2\pi f_0$). The phase angle of Co_3O_4 nanospheres was found to be -72°, which is close to 90° demonstrating its good capacitance response with ultrafast kinetic ability. Here, t_0 value equals 2.57 ms which means that the maximum

capacitance could be reached in an ultrafast charge time (Nashim *et al.* 2021).
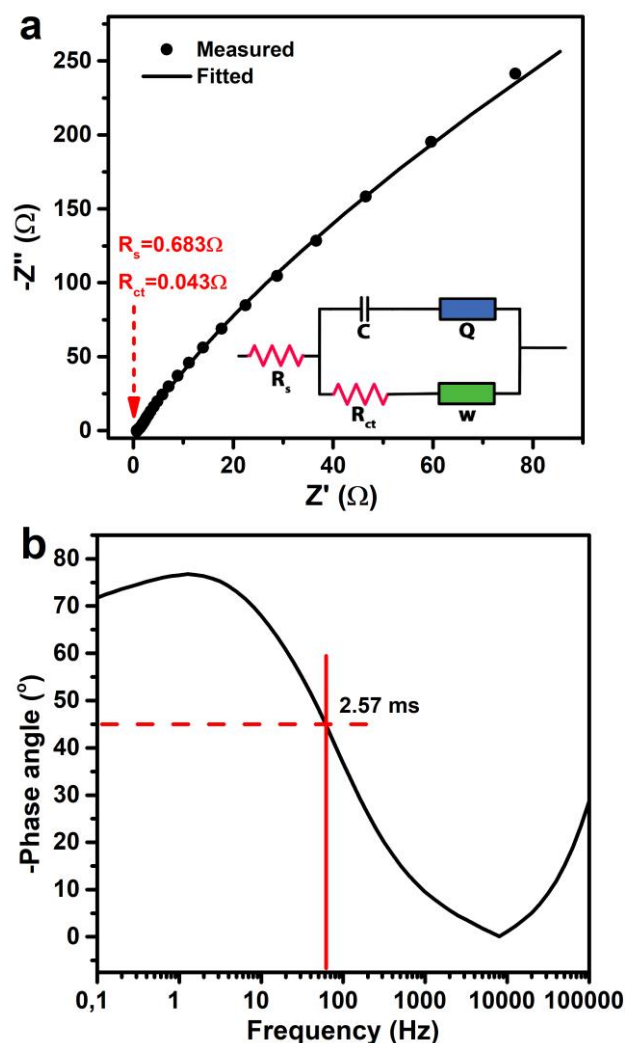
Fig. 8. (a) Nyquist plot (The inset shows the equivalent circuit) and **(b)** Bode diagram.

Table 2. Specific capacitances obtained from different methods in a three-electrode system.

Cyclic voltammetry (CV)		Galvanostatic charge/discharge (GCD)	
Scan rate (mV/s)	Specific Capacitance (F/g)	Current Density (A/g)	Specific Capacitance (F/g)
10	285	0.5	171
25	261	1	159
50	235	2	132
100	201	3	121
200	155	5	108

4. Conclusion

In summary, cobalt oxide nanospheres were fabricated by an easy (one-step) and ultrafast (only 5 minutes) in molten KNO_3-salt method and were analyzed by SEM, EDX, TEM, XRD, and FTIR techniques. When applied as the electrode material, a specific capacitance of 285 F/g and 171 F/g were found at 10 mV/s and 0.5 A/g, respectively. The electrode exhibited a moderate rate capability (63.1% at 5 A/g) and had good cyclic stability (90.5% after 1200 cycles). Anyway, this efficient fabrication approach is so simple, thus easily can be extended for the fabrication of various metal oxides without complicated operations.

5. References

Afrooze, A., and Shaik D., 2023. Porous Co_3O_4 Nanospheres Synthesized via Solution Combustion Method for Supercapacitors. *Chemical Papers, 77*, 1201–1211.

Anuradha, C.T., and Raji, P., 2022. Hydrothermal Synthesis, Characterization, and Electrochemical Behaviour of Cobalt Oxide Co_3O_4 Nanoparticles for Stable Electrode with Enhanced Supercapacitance. *Brazilian Journal of Physics*, **52,** 211-215.

Ardizzone, S., Fregonara G., and Trasatti S., 1990. Inner and Outer Active Surface of RuO_2 Electrodes. *Electrochimica Acta, 35,* 263–267.

Arjunan, A., Ramasamy S., Kim J., and Kim S.K., 2023. Co_3O_4 Nanoparticles-Embedded Nitrogen-Doped Porous Carbon Spheres for High-Energy Hybrid Supercapacitor Electrodes. *Journal of Energy Storage, 68*, 107758.

Chen, M., Ge Q., Qi, M., Liang X., Wang F., and Chen, Q., 2019. Surface & Coatings Technology Cobalt Oxides Nanorods Arrays as Advanced Electrode for High Performance Supercapacitor. *Surface & Coatings Technology*, **360,** 73–77.

Du, P., Dong Y., Dong Y., Wang X., and Zhang H., 2022. Fabrication of Uniform MnO_2 Layer-Modified Activated Carbon Cloth for High-Performance Flexible Quasi-Solid-State Asymmetric Supercapacitor. *Journal of Materials Science, 57,* 3497–3512.

Gao, W., Zhao Y., Chen W., Zhuang J., Shang M., Sun D., and Xie A., 2023. From Plastic to Supercapacitor Electrode Materials: Preparation and Properties of Cobalt Oxide/Carbon Composites with Polyethylene Terephthalate as Carbon Source. *Ceramics International*, **49 (5),** 7266–7273.

Guo, D., Song X., Li F., Tan L., Ma H., Zhang L., and Zhao Y., 2018. Oriented Synthesis of Co_3O_4 Core-Shell Microspheres for High-Performance Asymmetric Supercapacitor. *Colloids and Surfaces A: Physicochemical and Engineering Aspects*, **546,** 1–8.

Jadhav, S., Jadhav A., Mandlekar B., Sarawade P., and Anamika V., Kadam A., 2023. Influence of Deposition Current and Different Electrolytes on Charge Storage Performance of Co_3O_4 Electrode Material. *Journal of Physics and Chemistry of Solids, 180,* 111422.

Kebabsa, L., Kim J., Lee D, and Lee B., 2020. Highly Porous Cobalt Oxide-Decorated Carbon Nanofibers Fabricated from Starch as Free-Standing Electrodes for Supercapacitors. *Applied Surface Science,* **511,** 145313.

Kim, B.H., Yang K.S., and Yang D.J., 2013. Electrochemical Behavior of Activated Carbon Nanofiber-Vanadium Pentoxide Composites for Double-Layer Capacitors. *Electrochimica Acta*, **109,** 859–865.

Kurtan, U. 2022. Uniformly Decorated Nanocubes in Carbon Nanofibers for a Supercapacitor with Ultrahigh Cyclability and Stability. *Journal of Electronic Materials, 51*, 5159–5168.

Kurtan, U. and Aydın H., 2021. Introducing Organic Metallic Salts to Enhance Capacitive Energy Storage of Carbon Nanofibers. *Journal of Energy Storage*, **42,** 103016.

Lee, S.W., Gallant B., Byon H.R, Hammond P.T, and Shao-Horn Y., 2011. Nanostructured Carbon-Based Electrodes: Bridging the Gap between Thin-Film Lithium-Ion Batteries and Electrochemical Capacitors. *Energy & Environmental Science*, **4,** 1972–1985.

Liang, K., Tang X., and Hu W., 2012. High-Performance Three-Dimensional Nanoporous NiO Film as a Supercapacitor Electrode. *Journal of Materials Chemistry*, **22,** 11062–11067.

Lima-Tenório M.K., Ferreira C.S., Rebelo QHF., Souza

R.F.B., Passos R.R., Pineda E.A.G., and Pocrifka L.A., 2018. Pseudocapacitance Properties of Co₃O₄ Nanoparticles Synthesized Using a Modified Sol-Gel Method. *Materials Research*, **21**, e20170521.

Liu, F., Su H., Jin L., Zhang H., Chu X., and Yang W., 2017. Facile Synthesis of Ultrafine Cobalt Oxide Nanoparticles for High-Performance Supercapacitors. *Journal of Colloid and Interface Science,* **505**, 796–804.

Liu, M.C., Kong L.B., Lu C., Li X. M., Luo Y.C., and Kang L., 2012. A Sol – Gel Process for Fabrication of NiO/ NiCo₂O₄/Co₃O₄ Composite with Improved Electrochemical Behavior for Electrochemical Capacitors. *ACS Appl. Mater. Interfaces,* **4,** 4631–4636.

Ma, C., Wu L., Dirican M., Cheng H., Li J., Song Y., Shi J., and Zhang X., 2020. ZnO-Assisted Synthesis of Lignin-Based Ultra-Fine Microporous Carbon Nanofibers for Supercapacitors. *Journal of Colloid and Interface Science,* **586,** 412-422.

Meher, S.K., Justin P., and Rao G.R., 2011. Microwave-Mediated Synthesis for Improved Morphology and Pseudocapacitance Performance of Nickel Oxide. *ACS Applied Materials & Interfaces*, **3,** 2063–2073.

Nashim, A., Pany S., and Parida K.M., 2021. Systematic Investigation on the Charge Storage Behavior of GdCrO₃ in Aqueous Electrolyte. *Journal of Energy Storage*, **42**, 103145.

Packiaraj, R., Devendran P., Venkatesh K.S., Bahadur S.A., Manikandan A., and Nallamuthu N., 2019. Electrochemical Investigations of Magnetic Co₃O₄ Nanoparticles as an Active Electrode for Supercapacitor Applications. *Journal of Superconductivity and Novel Magnetism,* **32**, 2427–2436.

Pore, O. C., Fulari A. V, Kamble R. K., Shelake A. S., Velhal N. B., Fulari V. J., and Lohar G. M., 2021. Hydrothermally Synthesized Co₃O₄ Microflakes for Supercapacitor and Non-Enzymatic Glucose Sensor. *Journal of Materials Science: Materials in Electronics,* **32,** 20742–20754.

Priyadharsini, C. I., Marimuthu G., Pazhanivel T., Anbarasan P. M., Aroulmoji V., Siva V., and Mohana L., 2020. Sol–Gel Synthesis of Co₃O₄ Nanoparticles as an Electrode Material for Supercapacitor Applications. *Journal of Sol-Gel Science and Technology*, **96**, 416–422.

Tan, Y., Gao Q., Yang C., Yang K., Tian W., and Zhu L., 2015. One-Dimensional Porous Nanofibers of Co₃O₄ on the Carbon Matrix from Human Hair with Superior Lithium Ion Storage Performance. *Scientific Reports,* **5,** 12382.

Tharasan, P., Somprasong M., Kenyota N., Kanjana N., Maiaugree W., Jareonboon W., and Laokul P., 2022. Preparation and Electrochemical Performance of Nanostructured Co₃O₄ Particles. *Journal of Nanoparticle Research*, **24**, 126.

Tummala, R., Guduru R.K., and Mohanty P.S., 2012. Nanostructured Co₃O₄ Electrodes for Supercapacitor Applications from Plasma Spray Technique. *Journal of Power Sources*, **209**, 44–51.

UmaSudharshini, A., Bououdina M., Venkateshwarlu M., Dhamodharan P., and Manoharan C., 2021. Solvothermal Synthesis of Cu-Doped Co₃O₄ Nanosheets at Low Reaction Temperature for Potential Supercapacitor Applications. *Applied Physics A*, **127**, 353.

Üstün, B., Aydın H., Koç S.N., and Kurtan Ü., 2023. Electrospun Amorphous CoOₓ/C Composite Nanofibers Doped with Heteroatoms for Symmetric Supercapacitors. *Fuel*, **341**, 127735.

Vidhyadharan, B., Zain N.K.M, Misnon I.I., Aziz R.A., Ismail J., Yusoff M.M., and Jose R., 2014. High Performance Supercapacitor Electrodes from Electrospun Nickel Oxide Nanowires. *Journal of Alloys and Compounds*, **610**, 143.

Wang, D., Wang Q., and Wang T., 2011. Morphology-Controllable Synthesis of Cobalt Oxalates and Their Conversion to Mesoporous C Co₃O₄ Nanostructures for Application in Supercapacitors. *Inorganic Chemistry,* **50**, 6482–6492.

Wang, H.Q., Li Z.S., Huang Y.H., Li Q.Y., and Wang X.Y., 2010. A Novel Hybrid Supercapacitor Based on Spherical Activated Carbon and Spherical MnO₂ in a Non-Aqueous Electrolyte. *Journal of Materials Chemistry*, **20,** 3883–3889.

Wang, L., Duan G., Zhu J., Chen S. M., Liu X., and Palanisamy S., 2016. Mesoporous Transition Metal

Oxides Quasi-Nanospheres with Enhanced Electrochemical Properties for Supercapacitor Applications. *Journal of Colloid and Interface Science,* **483,** 73–83.

Yang, W., Gao Z., Ma J., Wang J., Wang B., and Liu L., 2013. Effects of Solvent on the Morphology of Nanostructured Co₃O₄ and Its Application for High-Performance Supercapacitors. *Electrochimica Acta,* **112,** 378–385.

Zhang, Z. J., Chen X.Y., Xie D.H., Cui P., and Liu J.W., 2014. Temperature-Dependent Structure and Electrochemical Performance of Highly Nanoporous Carbon from Potassium Biphthalate and Magnesium Powder via a Template Carbonization Process. *Journal of Materials Chemistry A*, **2,** 9675–9683.